

PAPER • OPEN ACCESS

## In-Flight Performance of the OCO-2 Cryocooler

To cite this article: Arthur Na-Nakornpanom *et al* 2015 *IOP Conf. Ser.: Mater. Sci. Eng.* **101** 012024

View the [article online](#) for updates and enhancements.

You may also like

- [Assessing progress toward the Paris climate agreement from space](#)  
Brad Weir, Tomohiro Oda, Lesley E Ott et al.
- [Anthropogenic CO<sub>2</sub> emissions assessment of Nile Delta using XCO<sub>2</sub> and SIF data from OCO-2 satellite](#)  
Ankit Shekhar, Jia Chen, Johannes C Paetzold et al.
- [Five years of variability in the global carbon cycle: comparing an estimate from the Orbiting Carbon Observatory-2 and process-based models](#)  
Zichong Chen, Deborah N Huntzinger, Junjie Liu et al.



**ECS**  
The  
Electrochemical  
Society  
Advancing solid state &  
electrochemical science & technology

**DISCOVER**  
how sustainability  
intersects with  
electrochemistry & solid  
state science research

# In-Flight Performance of the OCO-2 Cryocooler

Arthur Na-Nakornpanom, Bret J. Naylor and Richard A. M. Lee

Jet Propulsion Laboratory, California Institute of Technology, Pasadena, CA 91109  
USA

E-mail: arthur.na-nakornpanom@jpl.nasa.gov

**Abstract.** The Orbiting Carbon Observatory-2 (OCO-2) will have completed its first year in space on July 2, 2015. The OCO-2 instrument incorporates three bore-sighted, high-resolution grating spectrometers, designed to measure the near-infrared absorption of reflected sunlight by carbon dioxide and molecular oxygen. The cryocooler system design is coupled with the instrument's thermal control design to maximize the instrument's performance. A single-stage NGAS pulse tube cryocooler provides refrigeration to three focal plane arrays to ~120 K via a high conductance flexible thermal strap. A variable conductance heat pipe (VCHP) based heat rejection system (HRS) transports waste heat from the instrument located inside the spacecraft to the space-viewing radiators. The HRS provides tight temperature control of the optics to 267 K and maintains the cryocooler at 300 K. Soon after entering the A-Train on August 3, 2014, the optics and focal planes were cooled to their operating temperatures. This paper provides a general overview of the cryogenic system design and reviews the in-flight cryogenic performance during the Observatory's first year.

## 1. Introduction

The primary science objective of the Orbiting Carbon Observatory-2 (OCO-2) is to collect space-based measurements of atmospheric carbon dioxide with the precision, resolution and coverage needed to characterize its sources and sinks and quantify their variability over the seasonal cycle. These measurements will improve our ability to forecast CO<sub>2</sub> induced climate change. During its two-year mission, OCO-2 will fly in a sun-synchronous, near-polar orbit in front of a group of Earth-orbiting satellites, with related carbon cycle science objectives whose ascending node crosses the equator near 13:30 hours Mean Local Time. Near-global coverage of the sunlit portion of Earth is provided in this orbit over a 16-day repeat cycle.

The OCO-2 instrument, designed and built by the Jet Propulsion Laboratory (JPL) for NASA, uses three high-resolution diffraction grating spectrometers to measure the gas concentrations at three wavelength bands (1.60  $\mu\text{m}$  Weak CO<sub>2</sub>, 2.06  $\mu\text{m}$  Strong CO<sub>2</sub> and 0.76  $\mu\text{m}$  O<sub>2</sub> A-band) from sunlight reflected off the Earth's continents and oceans through a column of air in the atmosphere. By measuring CO<sub>2</sub> concentrations over time at the same location, OCO-2 will be able to track sources and sinks on regional scales. To reduce thermally induced measurement errors, the one silicon (HyViSi) and two mercury cadmium telluride (HgCdTe) focal plane arrays (FPAs) must remain at a cold and stable temperature. The three FPAs are cooled to ~120 K by means of a single cryocooler, maintaining its cold block at  $110 \pm 0.05$  K, such that the FPAs remain stable to within  $\pm 0.1$  K per 98 minute orbit.



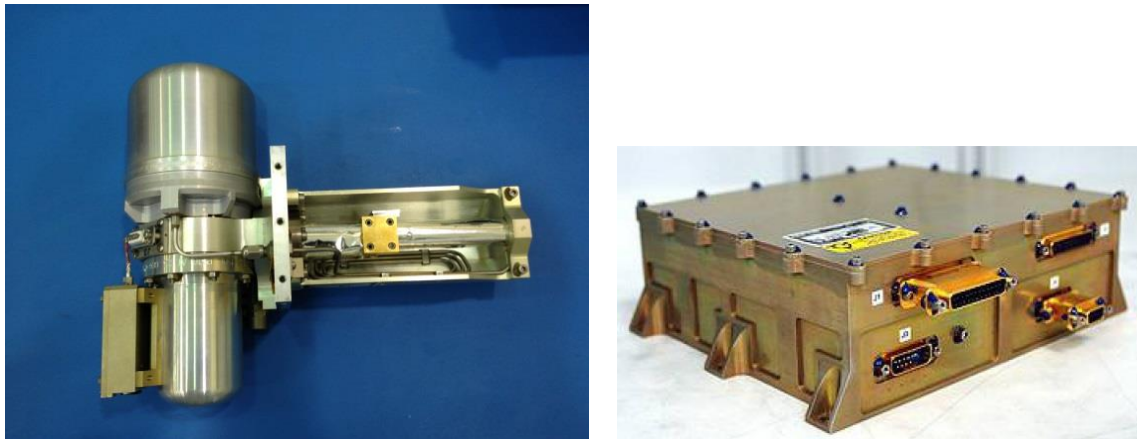


**Figure 1.** NGAS High Efficiency Cryocooler (HEC) and Advanced Cryocooler Electronics (ACE).

The OCO-2 cryocooler system consists of the elements shown in figure 1, including the Thermal Mechanical Unit (TMU) and the Cryocooler Control Electronics (CCE). The TMU is the Northrop Grumman Aerospace Systems (NGAS) High Efficiency Cryocooler (HEC), which is a single stage linear pulse tube cooler. The CCE is the NGAS Advanced Cryocooler Electronics (ACE), which provides power and control to the cryocooler. Extensive characterization of the OCO-2 cryocooler system was carried out during development and qualification testing phases at NGAS and JPL, followed by integration and testing of the cryocooler system at both the instrument and observatory levels [1].

The cryogenic subsystem (CSS), as shown in figure 2, provides the interface between the three FPAs and the TMU. The CSS was designed, manufactured and tested by Space Dynamics Laboratory (SDL). The CSS consists of three subassemblies, one for each FPA, and a flexible aluminum foil thermal link that connects each subassembly to the TMU. Each subassembly provides a mounting location for an FPA, while thermally isolating each FPA from the instrument optical bench and thermally coupling the FPAs to the TMU cold block. The FPA mounts consist of reentrant tri-fold G10 fiberglass/epoxy tube construction and MLI to minimize parasitic heat loads on the FPAs. The cryocooler beginning-of-life (BOL) heat load is approximately 3 W at 110 K. With the TMU cold block controlled to 110 K, the CSS maintains the three FPAs near the desired temperature of 120 K.

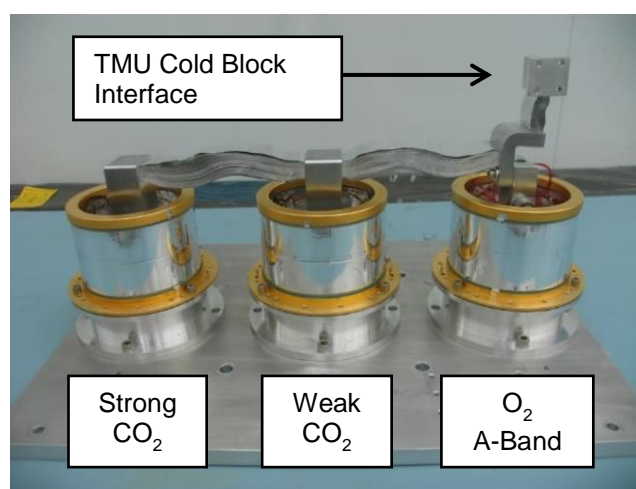


**Figure 2.** SDL Cryogenic Subsystem (CSS).

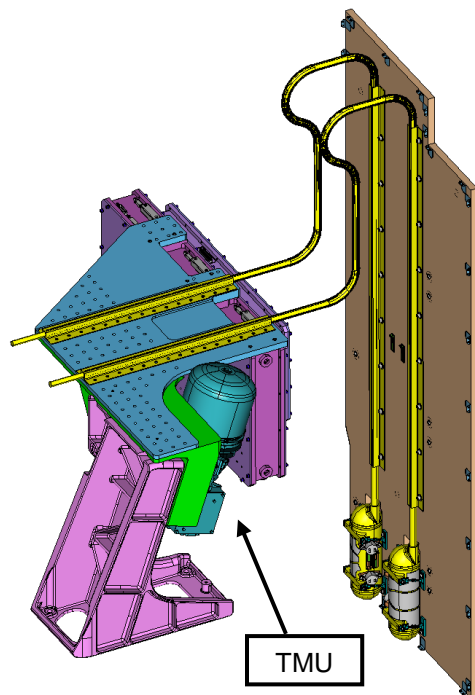


**Figure 3.** Cryocooler Heat Rejection System (HRS).

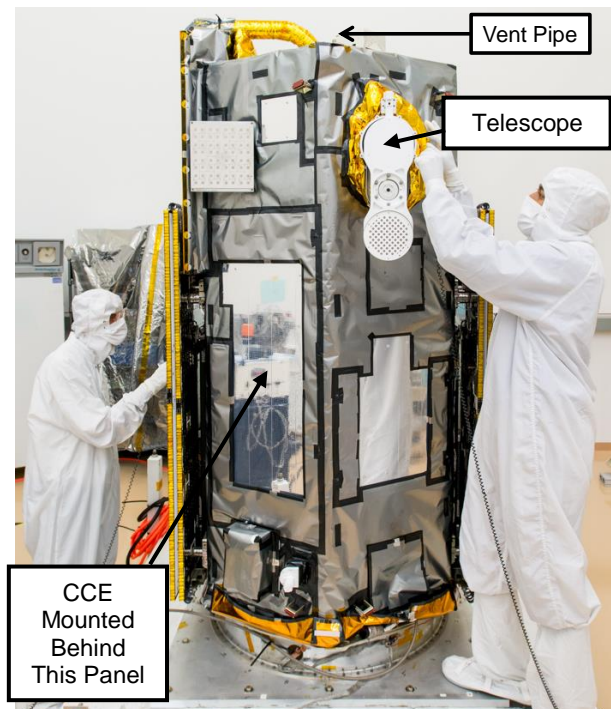


**Figure 4.** Orbiting Carbon Observatory-2 (OCO-2).

The waste heat from the cryocooler is removed by means of a heat rejection system (HRS) that utilizes two variable conductance heat pipes (VCHPs) and a space viewing radiator, as illustrated in figure 3. The condenser sections of the VCHPs are bonded and fastened to the radiator, and the evaporator sections are attached to an aluminum thermal plane, which interfaces to the cryocooler. A closed-loop heater controller, with the heater located at the reservoir and a temperature sensor at the evaporator, control the cryocooler heat rejection temperature to within  $\pm 0.3$  K.

The LEOStar-2 spacecraft bus, provided by Orbital Sciences ATK, is made primarily of aluminum honeycomb panels that form a hexagonal structure approximately 1 meter in diameter and 2 meters tall, as shown in figure 4. The Earth-viewing honeycomb panels structurally support and remove waste heat from spacecraft components, instrument electronics, and the CCE. A set of momentum wheels onboard the spacecraft points the instrument telescope in three primary observatory operating modes: directly downwards towards the Earth's landmass in Nadir Mode, at the sun's reflection off the Earth's oceans in Glint Mode and at a specific location on the Earth in Target Mode. A complete description of the thermal control system of the instrument is provided elsewhere [2].

## 2. Initial In-Flight Performance

OCO-2 successfully launched on July 2, 2014 aboard a Delta II launch vehicle from Vandenberg Air Force Base in California. On day 2, the observatory transitioned from Survival Mode to Nadir Mode, and both the instrument and decontamination heaters were powered on to raise the FPAs and optical bench to 300 K. The CCE was powered on during day 5 (July 6, 2014) to verify the health of the cryocooler system and complete the instrument initial checkout.

Following launch, the OCO-2 instrument was subjected to a 32 day decontamination period to allow time for the moisture in the instrument structure and MLI to dissipate away from the CSS, into the instrument shroud volume, and out through the aluminum vent pipe into space. To end the decontamination period and prepare the instrument for cool down, the instrument decontamination heaters were turned off on day 34 (August 4, 2014).

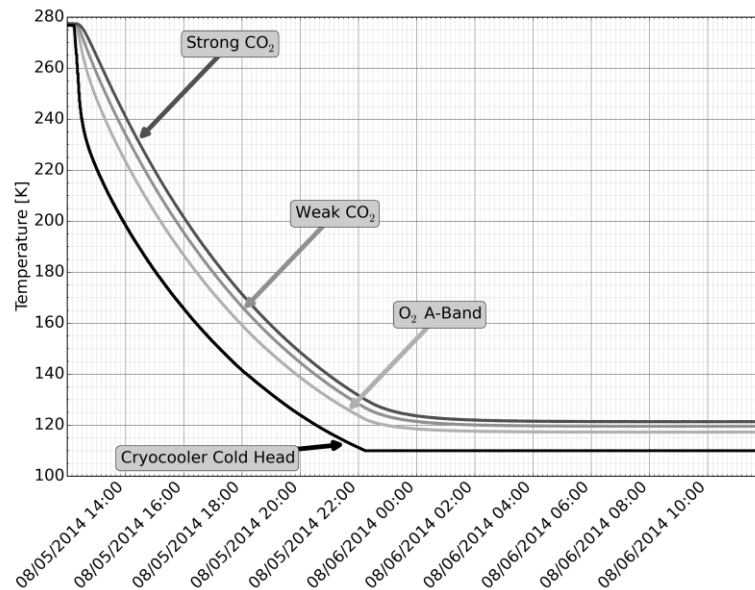


**Figure 5.** Initial In-Flight Cooldown of the FPAs and Cryocooler Cold Head.

On day 35 (August 5, 2014), the TMU was powered on as shown in figure 5, with the FPAs starting at a slightly lower temperature than previous cooldowns during ground testing. At BOL, the cryocooler compressor was operating at 31 W on day 36. The initial water accumulation rate at BOL resulted in the TMU drive level increasing at a rate of 0.62% per day. Due to the science requirement of maintaining the FPAs at  $\sim 120$  K, the TMU cold head setpoint was decreased from 110 K to 106.8 K on day 43 (August 13, 2014) as shown in figure 6, resulting in the motor power increasing from 39 W to 42 W as shown in figure 7. The FPAs continued to drift out of range, resulting in another TMU cold head setpoint change from 106.8 K to 105.7 K on day 57 (August 27, 2014), resulting in a motor power increase from 44.4 W to 45.6 W.

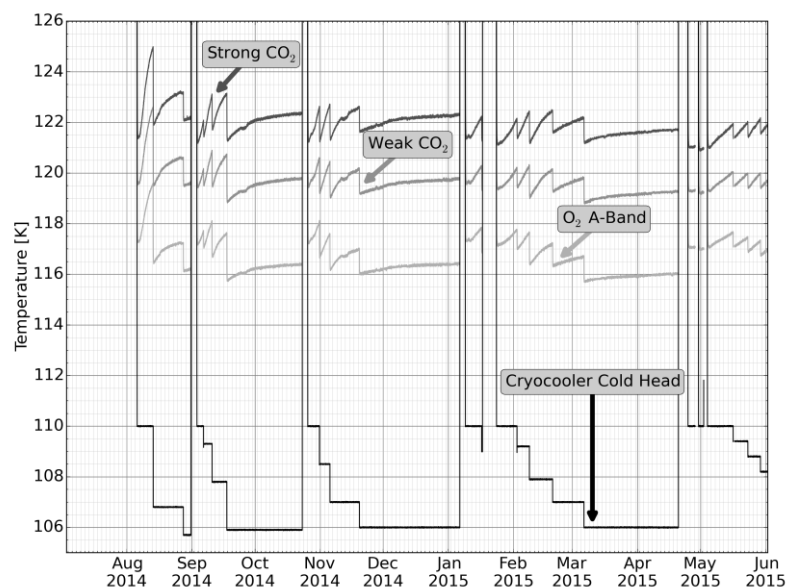


**Figure 6.** In-Flight TMU Cold Head and FPA Temperatures.

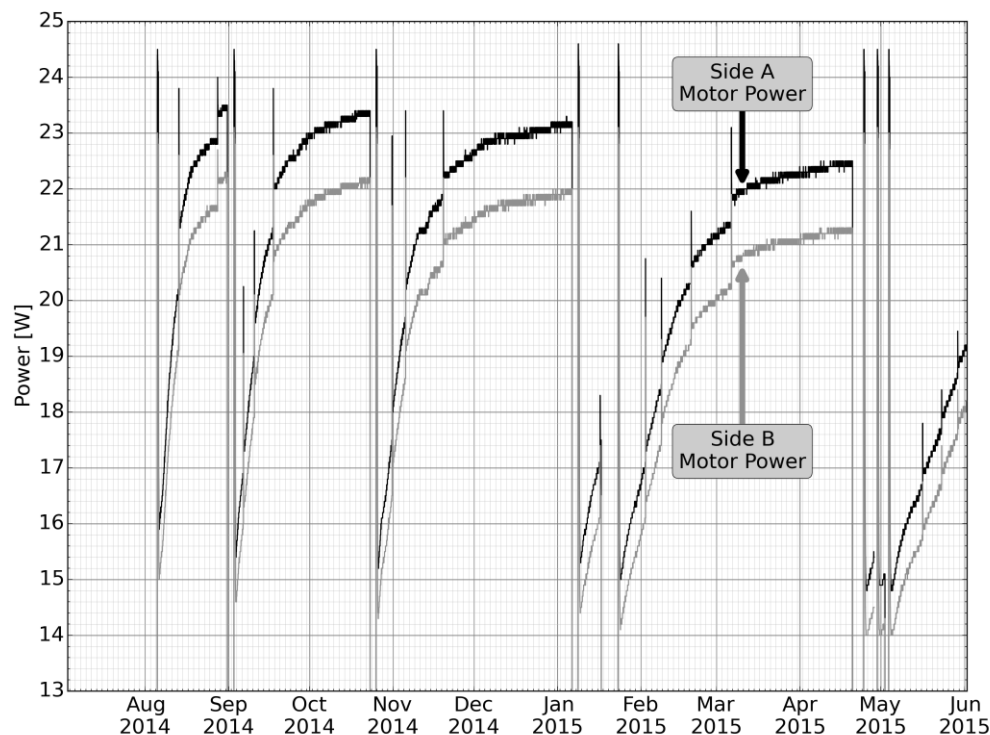


**Figure 7.** In-Flight TMU Motor Power.

### 3. De-Icing Results

During the mission, science measurements need to be interrupted due to the need to decontaminate as a result of water cryodepositing onto the cold surfaces of the CSS [3]. The water contamination increases the thermal heat load, which in turn leads the cryocooler motor drive level to approach its user-programmable maximum limit of 50%. Prior to launch, it was known that periodic decontamination cycles would be required over the life of the mission, and that this need would decrease over time. Due to limitations in the spacecraft bus power budget, the TMU is limited to a maximum of 48 W compressor power, which is equivalent to 50% motor drive level.

With the TMU drive level increasing at a rate of 0.04% per day, the 50% limit would be reached by day 70. The first de-ice cycle was started on day 61 (August 31, 2014), with the turning off of the TMU, followed by turning on the FPA decontamination heater to dwell the CSS at 285 K, in order to drive off any accumulated water out through the instrument vent pipe. After two days of de-icing, the decontamination heater was turned off on day 63 (September 2, 2014). The TMU was restarted to bring the cold head back down to 110 K, and the motor power reached a minimum of 30 W on day 64, an improvement from the initial BOL level of 31 W on day 36.

Figure 6 shows the TMU cold head and FPA temperatures for the first ten months of cooler operation. After each de-ice cycle, the cold head setpoint needs to be decreased in steps in order to maintain the FPAs at  $\sim 120$  K. Figure 7 shows the TMU motor power for the first ten months of cooler operation. The second de-ice cycle was started on day 114 (October 23, 2014) again due to indications that the 50% drive limit would be reached. After two days of de-icing, the decontamination heater was turned off and the TMU was restarted, with the motor power reaching a minimum of 29.6 W on day 117, a slight improvement from the 30 W observed on day 64.

Figure 8 clearly shows that the level of icing has decreased over time after each de-ice cycle. The requirement for a de-ice cycle is now driven by gain degradation in the  $O_2$  A-band detector, not due to the 50% drive limit. The third de-ice cycle was started on day 189 (January 6, 2015) and the fourth de-ice cycle started on day 293 (April 20, 2015).



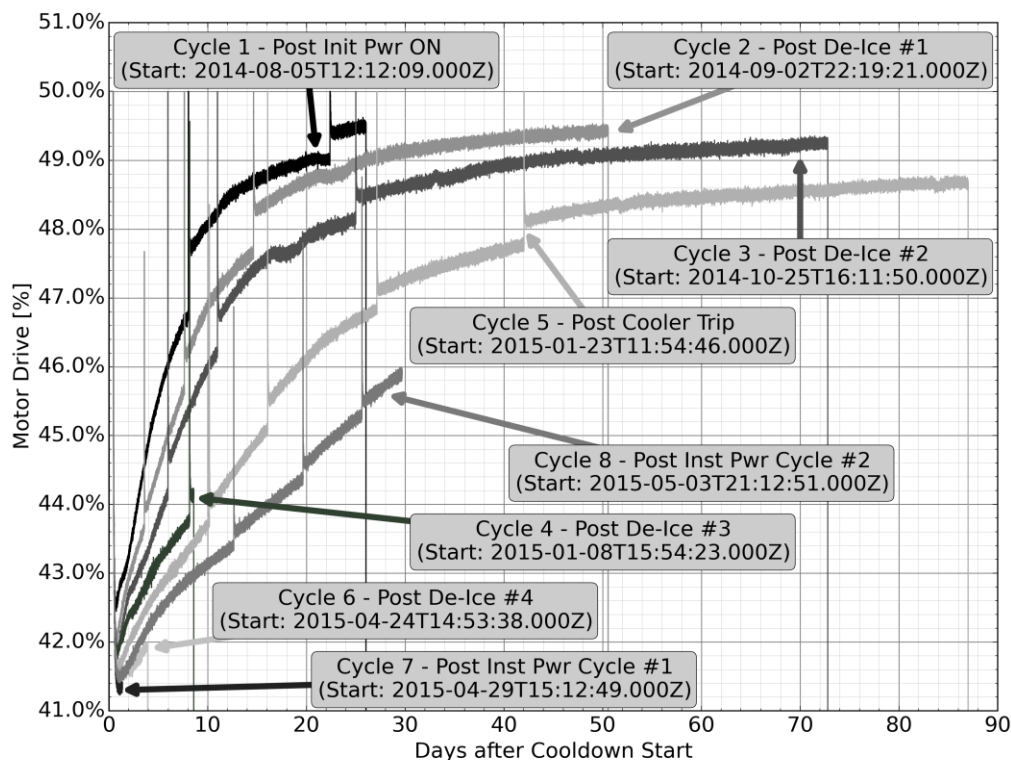


**Figure 8.** In-Flight TMU Motor Drive Performance Comparison.

#### 4. Cryocooler Accelerometer Overload Trip Out

The TMU unexpectedly tripped off on day 200 (January 17, 2015) due to an accelerometer overload fault. The accelerometer overload detector is intended to protect the TMU against over-stroking. It does not differentiate between internal cooler vibration and external vibration, and can be false alarmed by external mechanical noise. This type of trip had been observed during cryocooler and instrument ground testing, where the cause was attributed to external sources such as vibrating heat exchanger chiller lines or ground support equipment movement around the test chamber. In the interest of returning OCO-2 back to science mode, it was determined that there was no risk to powering on the TMU with the accelerometer overload trip function remaining enabled. This trip event provided the opportunity to perform a de-ice cycle. After six days of de-icing, the TMU was powered on day 206 (January 23, 2015) and the cryocooler system has operated normally to date.

The root cause investigation and corrective action still remained open, due to the risk that a similar trip could reoccur. Analysis of cryocooler telemetry showed that the TMU had been operating normally up to the time of the event. There were no unique instrument or spacecraft activities at the time of the trip, and the space environment was not abnormal. The accelerometer overload detector threshold is set to 47 mG, however the RSS of the first 16 harmonics at the time of the trip was 4.1 mG RMS.

After a thorough investigation, the root cause could not be identified, and the event was deemed to be a false trip. The CCE provides several layers of protection against over-stroke; asynchronous time-domain accelerometer overload detection, synchronous frequency-domain individual harmonic over-vibration detection, motor over-current detection and motor drive limit. Since the risk was very low due to the other layers of protection in place, it was decided to implement the corrective action of disabling the accelerometer overload detector on day 306 (May 3, 2015) to eliminate the risk of future false alarms. There have been no subsequent cryocooler faults of any kind to date.

## 5. Instrument Trip Outs

The spacecraft fault detection system unexpectedly tripped off the instrument digital processors (DPs) and analog front-end electronics (AFE) on day 299 due to an error in the observatory autonomous time sequence (ATS). The ATS is used to command the observatory autonomously. The ATS was expected to open the instrument telescope door before exiting eclipse with nominal fault protection in place, allowing the instrument to see the sunlit Earth. However, the ATS incorrectly had solar polar calibration (SPC) fault protection enabled, thus when OCO-2 exited eclipse with the door open, an SPC fault occurred, resulting in an unnecessary shut-down of the instrument DPs and AFE for protection. It was therefore necessary to power cycle the instrument, in order to reset it to its nominal state, which provided the opportunity to perform another de-ice cycle. After one day of de-icing, the TMU was powered on during day 302 (April 29, 2015).

However, as the instrument was recovering on day 302, the spacecraft fault detection system again unexpectedly tripped off the instrument DPs and AFE due to an error in the instrument power cycle sequence that was overlooked. Again, the instrument fault protection was incorrectly enabled and the DPs and AFE powered off for protection. The instrument had to be power cycled again, providing another opportunity to perform a de-ice cycle. After one day of de-icing, the TMU was powered on during day 306 (May 3, 2015). There have been no subsequent instrument faults of any kind to date.

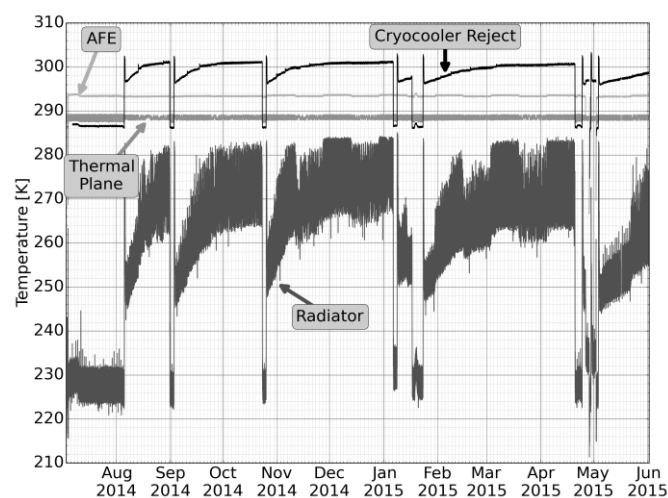


**Figure 9.** In-Flight Cryocooler HRS Temperatures.

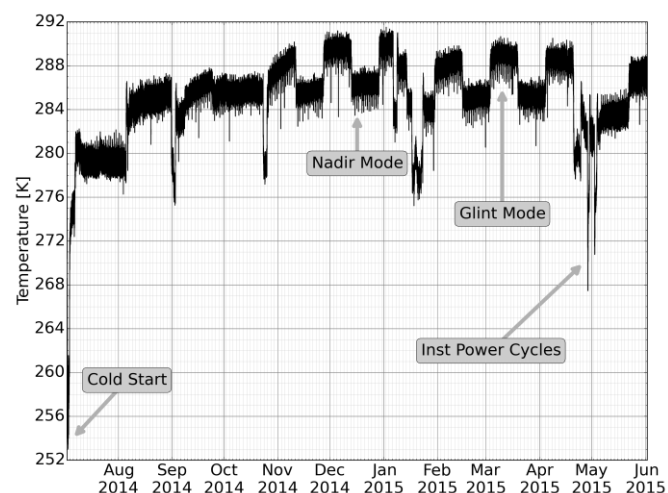


**Figure 10.** In-Flight CCE Rejection Temperature.



## 6. Heat Rejection System Performance

The HRS for the cryocooler has performed exceptionally well and maintained the cryocooler within its nominal temperature range as shown in figure 9. When the cryocooler is turned on, its baseplate reaches a maximum temperature of 303 K during cooldown. The baseplate is maintained at an average temperature of 300 K when the cryocooler is in stable operation. When the cryocooler is turned off, the HRS maintains the baseplate at an average temperature of 286 K. The heater control system on the VCHP HRS maintains the cryocooler rejection temperature variation to  $\sim 0.6$  K p-p while the radiator temperature varies by  $\sim 20$  K p-p.

Figure 10 details the CCE heat rejection temperature variation. The CCE endured a cold start at 253 K on day 5. When the CCE is operating nominally, the honeycomb spacecraft panel maintains the CCE at an average temperature of 285 K with an orbital temperature variation of  $\sim 3$  K p-p. The effect of the transitions between the 16 day Nadir and Glint Mode cycle on the spacecraft panels are clearly seen on the CCE. The two planned instrument power off/on cycles in late April 2015 and early May 2015 were performed in back-to-back orbits, to prevent the instrument from reaching survival temperatures, thus the CCE temperature was maintained well above 253 K.

## 7. Summary

The OCO-2 cryocooler system has performed exceptionally well to date. The ice contamination rate on the detectors and cryogenic surfaces has decreased over time such that de-icing cycles are now only performed once every four months. The heat rejection system for the cryocooler and CCE have performed well, maintaining the compressor and CCE near 300 K and 285 K, respectively. The performance of the cryocooler system has enabled OCO-2 to meet its science objectives and is expected to continue for the remainder of the two-year mission.

## Acknowledgments

The authors would like to thank the JPL OCO-2 team, as well as the subcontractors that contributed to the success of the OCO-2 cryocooler system, including Northrop Grumman Aerospace Systems in Redondo Beach, California, Space Dynamics Laboratory in Logan, Utah, and Orbital Sciences ATK in Dulles, Virginia and Gilbert, Arizona. The authors would especially like to recognize the support of the OCO-2 Project Manager, Dr. Ralph Basilio.

These data were produced by the OCO-2 Project at the Jet Propulsion Laboratory, California Institute of Technology, and obtained from the OCO-2 data archive maintained at the NASA Goddard Earth Science Data and Information Services Center.

## References

- [1] Na-Nakornpanom A, Johnson D and Naylor B 2015 OCO-2 cryocooler development, integration and test *18<sup>th</sup> International Cryocooler Conference (Syracuse, New York, 09-12 June 2014) (Cryocoolers 18)* (Boulder:ICC Press) pp 105-14
- [2] Rivera J, Rodriguez J and Johnson D Development of the OCO instrument thermal control system 2008 *38<sup>th</sup> SAE Tech. Paper Series (San Francisco, California)*
- [3] Ross R 2003 Cryocooler load increase due to external contamination of low- $\epsilon$  cryogenic surfaces *12<sup>th</sup> International Cryocooler Conference (Cambridge, Massachusetts, 18-20 June 2002) (Cryocoolers 12)* (New York:Plenum) pp 727-36
- [4] Rodriguez J, Collins S, Na-Nakornpanom A and Johnson D 2006 On-orbit performance of the TES pulse tube coolers and instrument – A first year in space *50<sup>th</sup> Cryogenic Engineering Conference (Keystone, Colorado, 29 Aug - 2 Sept 2005) (Advances in Cryogenic Engineering vol 51)* (New York:AIP) pp 1937-44
- [5] Ross R and Rodriguez J 2004 Performance of the AIRS pulse tube coolers and instrument – A first year in space *49<sup>th</sup> Cryogenic Engineering Conference (Anchorage, Alaska, 22-26 Sept 2003) (Advances in Cryogenic Engineering vol 49)* (New York:AIP) pp 1293-300